REPORT DOCUMENTATION PAGE

Form Approved
OMB No. 0704-0188

T DATE	3. REPORT TYPE AND DATES COVERED
29 Jun 91	Annual Report: 1Jun90-30May91

4. TITLE AND SUBTITLE

Wavelet Transforms and Parallel Image Processing

5. FUNDING NUMBERS

G:AFOSR-90-0310
PR/TA: 9806/00

6. AUTHOR(S)

Ching-Chung Li, M. Gökmen
Richard W. Hall

7. PERFORMING ORGANIZATION NAME(S) AND ADDRESS(ES)

University of Pittsburgh
Department of Electrical Engineering
348 BEH
Pittsburgh, PA 15261

8. PERFORMING ORGANIZATION REPORT NUMBER

TR-SP-91-05

9. SPONSORING/MONITORING AGENCY NAME(S) AND ADDRESS(ES)

DARPA-AFOSR/NM
Building 410
Bolling AFB DC 20332-6448

10. SPONSORING/MONITORING AGENCY REPORT NUMBER

AFOSR-90-0310

11. SUPPLEMENTARY NOTES

12a. DISTRIBUTION/AVAILABILITY STATEMENT

**Approved for public release;
distribution unlimited.**

12b. DISTRIBUTION CODE

13. ABSTRACT *(Maximum 200 words)*

A wavelet function generated by a specially constructed symmetric scale function has been explored for use in edge detection. Experiments showed that relatively refined edge information was obtained in the coarse resolution levels. An edge detection algorithm based on regularization with space-varying parameters has been developed, where the values of the parameters are adaptively determined iteratively. A multiscale edge detection algorithm using a first order regularization filter has been developed. It is demonstrated experimentally that the high localization performance of the filter is combined with high detection performance by using a multiscale integration scheme. Time performances have been evaluated for different embeddings of the wavelet coefficients into 2-D meshes over typical wavelet based algorithms. Parallel image processing algorithms are under study to identify fundamental parallel limits and to enable fully their parallel application in multiresolution applications. Novel graph compounds which can be utilized to enhance communication bandwidth in mesh architectures have been evaluated and appear to offer some promise in image processing.

14. SUBJECT TERMS

Wavelet Transforms, Image Processing, Edge Detection, Edge Integration, Regularization, Multiresolution Analysis, Parallel Computing Architectures, Parallel Algorithms

15. NUMBER OF PAGES

33

16. PRICE CODE

17. SECURITY CLASSIFICATION OF REPORT	18. SECURITY CLASSIFICATION OF THIS PAGE	19. SECURITY CLASSIFICATION OF ABSTRACT	20. LIMITATION OF ABSTRACT
UNCLASSIFIED	UNCLASSIFIED	UNCLASSIFIED	UL

NSN 7540-01-280-5500

Standard Form 298 (Rev. 2-89)
Prescribed by ANSI Std. 239-18

WAVELET TRANSFORMS AND PARALLEL IMAGE PROCESSING

TABLE OF CONTENTS

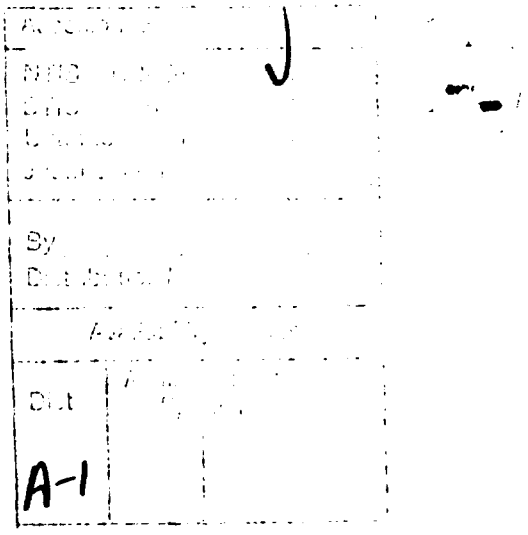

A. RESEARCH OBJECTIVES

1. Wavelet Transforms and Edge Detection

Approaches for integrating multiscale edge information using wavelet transforms shall be developed and these include the following endeavors:

a. Development of wavelet transforms for accurate edge detection.

b. Study of characteristic behaviors of edges in the wavelet representation.

c. Study of the connection between the regularization approach and the wavelet approach for edge detection, and development of a new wavelet transform using the derived connection.

d. Development of an approach for integration of wavelet-based multi-scale edges into a single level description for image segmentation.

e. Determination of values of the space-varying regularization parameters in the refined-regularization approach.

2. Parallel Image Processing

Computational issues which arise in the implementation of parallel image processing algorithms, with special emphasis on multiresolution approaches, shall be investigated. These issues include:

a. The determination and evaluation of desirable multiprocessor architectures with special emphasis on mesh based architectures.

b. The determination and evaluation of desirable embeddings of wavelet transform coefficients of 2-D images in the given architectures.

c. The implementation of parallel versions of the multiscale edge integration approaches identified in A.1.

d. The general study and development of parallel image processing algorithms for the architectures identified in A.2.a with special emphasis on algorithms using multiresolution image representations.

3. Experimental Program

Wherever possible the algorithms developed will be implemented on standard workstations (e.g. SUN-4) and will be evaluated with artificial and natural images. Further, those algorithms with meaningful parallel implementations will be implemented in simulated versions of architectures identified in A.2.a. in order to predict time performance in parallel realizations.

B. RESEARCH STATUS

B.1. Wavelet Transforms in Image Processing

B.1.a. Edge Detection Using Wavelet Transforms

The application of wavelet theory to multi-scale image processing has emerged as an exciting research problem during the past two years. The multi-resolution analysis allows an image to be studied at different scales; a scaled image at the resolution 2^{j-1} can be decomposed into the sum of the approximation at the lower scale (at resolution 2^{j}) and the difference image between the two scales which can be represented by the wavelet transform at the j^{th} scale. The edge informations are contained in the successive difference images, and the multi-scale edges can provide a detailed description of object boundaries. Several well-known wavelet bases functions have been explored for edge detection and image segementation ([MALL 89], [DAUB 88], [CHAN 90], [PENT 90]). In particular, Mallat and Zhong developed a spline wavelet and used wavelet maxima to characterize multi-scale edges ([MALL 89b], [MALL 90]). Daubechies orthonormal wavelets with compact support are very attractive for image coding and image processing ([DAUB 88], [ZETT 90]); when they are applied to edge detection, the detected edge location tend to be shifted by one pixel due to the fact that the scale function $\phi(x)$ is not a symmetric function and the wavelet function $\psi(x)$ is not anti-symmetric. In order to improve the edge localization, a wavelet was constructed on the basis of a set of values of Daubechies basis function (N=3), and its potential in edge detection has been experimentally explored. This is briefly discussed below.

Let us consider the one dimensional case and let $\phi_3(x)$ and $\psi_3(x)$ denote the Daubechie scale function and wavelet function respectively for index N=3. $\phi_3(x)$ has its peak at x=1 and its support in [0, 2N-1]. Let

$$f_3(x) = \frac{1}{2}\,[\phi_3\,(x + 1) + \phi_3(-x + 1)]$$

which is a symmetric function peaked at x=0 and has its support in [-4, 4]. However, $f_3(x)$ does not satisfy the 2-scale difference equation

$$f(x) = \sum_n c_n f(2x - n) \qquad \text{for all } x\varepsilon[-4, 4] \text{ and } n\varepsilon Z$$

thus, it cannot be used as a scale function. Instead, a symmetric scale function $\phi_s(x)$ is constructed such that

$$\phi_s(x) = \Sigma\, C_n \phi_s(2x - n) \qquad \text{for all } x\varepsilon[-4, 4]$$

$$\phi_s(x_k) = f_s(x_k) \qquad \text{for } x_k \varepsilon S$$

where S is a set of thirteen points (-4,-3,-2,-1.5,-1,-0.5,0, 0.5,1,1.5,2,3,4). The coefficients $\{C_n\}$ are related to the low-pass filter coefficients $\{h(n)\}$ where $h(n)=C_n/2$; the low-pass filter function is given by $H(\omega)=\Sigma_n h(n)\varepsilon^{-in\omega}$ which receives a signal at a given scale and produces a scaled signal at the next resolution level. A high-pass filter $G(\omega)=\Sigma_n g(n)\varepsilon^{-in\omega}$ can be chosen where

$$G(\omega) = -i\sqrt{1 - |H(\omega)|^2}\,\varepsilon^{-i\omega/2}\,\mathrm{sgn}(\omega)$$

whose output gives the wavelet transform. The filter coefficients $\{h(n)\}$ and $\{g(n)\}$ are given in Table 1.1.

Table 1.1 Filter Coefficients for the Given Wavelet Transform

n	h(n)	g(n)
-4	0.0171184109	-0.0122422692
-3	-0.0202565862	-0.0228800973
-2	-0.0595227389	0.0261126331
-1	0.2713073859	0.0373127434
0	0.5827070568	-0.4996226426
1	0.2713073859	0.4996226426
2	-0.0595227389	-0.0373127434
3	-0.0202565862	-0.0261126331
4	0.0171184109	0.0228800973
5	0	0.0122422692

The wavelet function $\psi(x)$ satisfies

$$\psi(x) = 2\Sigma_n\, g(n)\,\psi(2x - n)$$

Although $\phi_s(x)$ has a compact support [-4, 4], $\psi(x)$, however, is not compactly supported as shown in Fig. 1.1 (a) and (b) respectively. Note that the right half of $\phi(x)$, $x\varepsilon[0,4]$, is similar in shape to Daubechies $\phi_3(x)$ for $x\varepsilon[1,5]$, $\psi(x)$ is very different from Daubechies $\psi_3(x)$. Because of the anti-symmetry of $\psi(x)$ with respect to x=1/2, it may provide better capability for edge detection and localization.

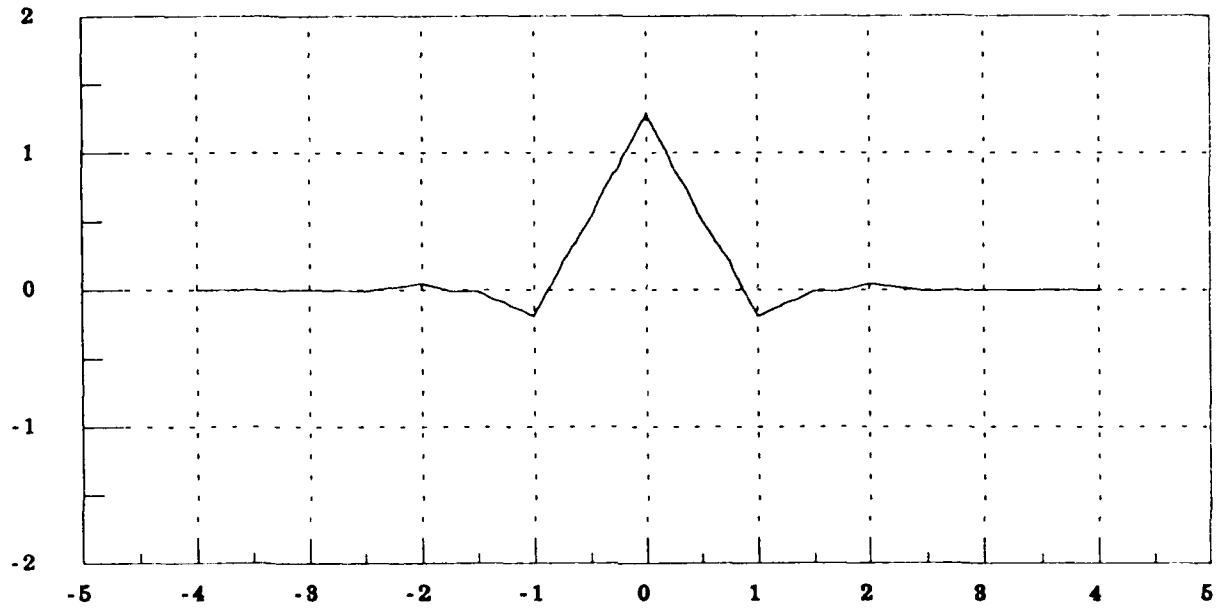

(a) $\phi_s(x)$

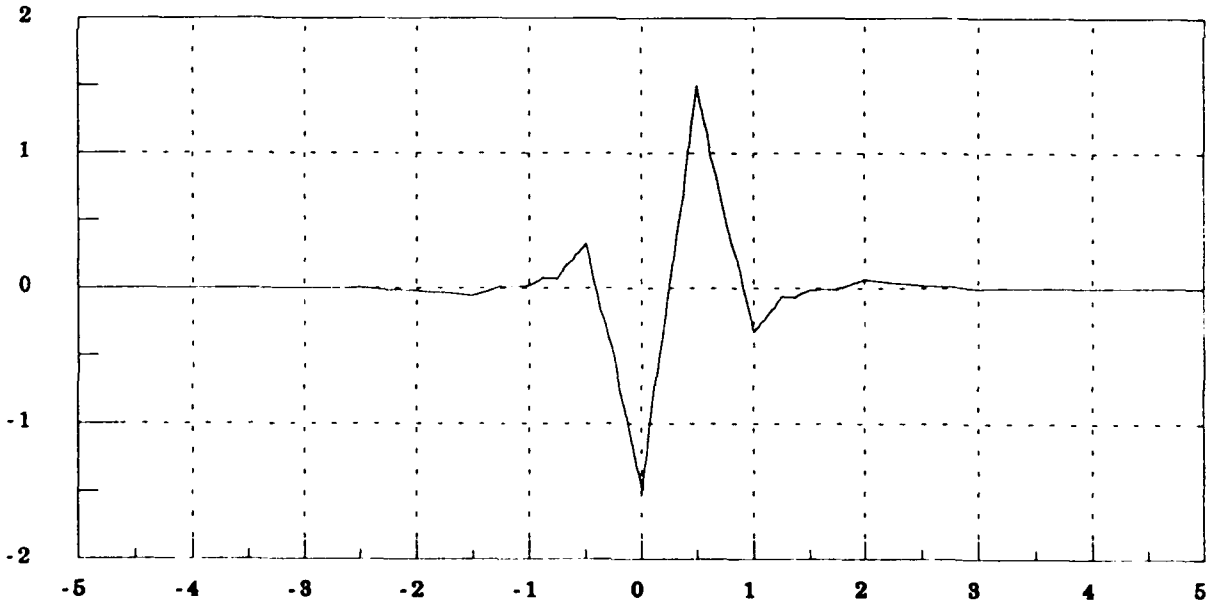

(b) $\psi(x)$

Figure 1.1 The constructed scale function $\phi(x)$ and wavelet function $\psi(x)$.

For two dimensional images, one can apply the one dimensional wavelet transform analysis first row-wise and then column-wise giving three subimages which contain directional edge informations between two consecutive scales; they may be merged into a single image by taking the maximum value at each pixel. Fig. 1.2 illustrates an experimental result on a girl's image (Lenna image), where the wavelet transforms (before taking wavelet maxima) at levels 1, 2, and 3 are shown together with the original image. As compared to Mallat and Zhong's wavelet transform, the magnitude of our wavelet transform at level 1 appears to be weaker but the relatively refined edge information was observed in level 3 which may facilitate the integration of multi-scale edges. More experimental work is in progress. The details will be described in our technical report TR-SP-91-06 which will be submitted in July 1991.

During the second year of the project period, studies on wavelet transforms for accurate localization will be continued. Barlaud's recent algorithm [BARL 91] will be taken into consideration. The connection between wavelet-based edge detection and the regularization-based multiscale edge detection will be studied as mentioned in the next section. Characteristic behaviors of edges [LUJA 89] [TAGA 90] in wavelet transforms will be examined. The performances of our developed algorithms will be evaluated and compared.

B.1.b. **Signal Characterization by Split Dyadic Wavelet Transform**

An extension of the dyadic wavelet transform, termed the split dyadic wavelet transform (SDWT), has been developed. It decomposes the dyadic wavelet transform at each scale into K information channels, where each channel is designed to characterize a specific feature in a digital signal f(n). The information channels may be constructed by using either linear or nonlinear operators T_k's on the dyadic wavelet transform $W_{2^j} f(n)$ and on the scaled signal $S_{2^j} f(n)$, where k denotes the k^{th} channel. A condition is

(a) Original image

(b) Level 1

(c) Level 2

(d) Level 3

Figure 1.2 The experimental result of applying the developed wavelet transform to the Lenna image.

imposed such that the sum of the outputs of these channels is equal to the original wavelet transform at each scale, i.e.,

$$W_{2^j} f(n) = \sum_{k=1}^{K} T_k [W_{2^j} f(n)]$$

and

$$S_{2^j} f(n) = \sum_{k-1}^{K} T_k [S_{2^j} f(n)] \ .$$

The SDWT has been applied to analyze some biological signals such as respiratory signals for accessing the pulmonary functions, where the respiratory tidal volume is digitally recorded with sampling rate of 64 Hz. The signal shows up-going trends correspond to inhaling and down-going trends correspond to exhaling. The fluctuations superimposed on the up-going and down-going trends carry important information about the physiological structure of breathing channels. A Gaussian wavelet was used; the nonlinear operator T_1 (associated with channel 1) is given by

$$T_1[W_{2^j} f(n)] = \begin{cases} W_{2^j} f(n), & \text{if } W_{2^j} f(n) > 0 \ ; \\ 0, & \text{otherwise} \end{cases}$$

T_2 (associated with channel 2) is the complement of T_1. The results of the five-scale wavelet analysis showed its potential application to estimate the air flow into and out of the lung, providing a new characterization and visualization of the signal. This work is described in our technical report TR-SP-91-03.

B.2. Edge Detection Using Regularization Theory

B.2.a. Edge Detection Using Refined Regularization

An edge detection algorithm based on regularization with space-varying parameters has been developed where the smoothness is controlled spatially over the image space. The assumption of the smoothness constraint in the global sense using a fixed regularization parameter is one of the major problems of the algorithms based on regularization theory. Several nonstandard algorithms have been developed to overcome these problems by using line process, but they suffer from the extensive computation required in minimizing the resulting nonconvex functionals. In this algorithm, the values of parameters in the model are adaptively determined by an iterative refinement process, hence the image dependent parameters such as the optimum value of the regularization parameter or the filter size are eliminated.

The algorithm starts with an oversmoothed regularized solution and iteratively refines the surface around discontinuites by using the structure around the discontinuities as exhibited in the error signal. The spatial control of smoothness is shown to resolve the conflict between detection and localization criteria of edge detection. The computational aspects of the algorithm as well as its performance on real and synthetic images were studied. This work is described in our technical report TR-SP-91-02 and has been presented to the 1991 IEEE Computer Society Conference on Computer Vision and Pattern Recognition.

B.2.b. **Multiscale Edge Detection Using First Order R-Filter**

A multiscale edge detection scheme using the regularization filter (R-filter) has been studied. The derivative of the first order R-filter obtained from the 1-D string functional favors the localization performance at the expense of relatively degraded detection performance. In order to improve the detection performance, edges at the different scales are combined by a simple integration scheme which is due in part to the improved localization performance of the R-filter at each stage. This operator minimizes the shift of edges in scale space, and simplifies the integration of the corresponding edges at successive scales. The properties of the filter as well as its relation with other edge operators have been examined. The combined edges from this multiscale representation have been evaluated by using both quantitative and qualitative measures for artificial and natural images. A brief summary of this work is given below. The details are described in our technical report TR-SP-91-04.

Multiscale Edge Operator

A multiscale representation may be obtained by carrying out the smoothing process using the regularization; each level of resolution is obtained by minimizing the string functional

$$E_m(f, \lambda) = \int_\Omega (f - d)^2 dx + \lambda \int_\Omega f_x^2 dx$$

where d is the image data and f is the regularized solution. The scale parameter in this case is the regularization parameter λ so that the coarse levels of representation are obtained by minimizing the string functional with a large λ, while fine levels are obtained by using a small λ. Sweeping the parameter λ continuously generates the scale space representation.

Let $V=\{v_1, v_2, \ldots, v_n\}$ be the set of images obtained by applying a smoothing operation to the image data with different degree of smoothing, and $W = \{w_1, w_2, \ldots, w_n\}$ be the set of images containing the gradient

information at each scale. For the Gaussian case, the set W can be constructed by convolving the signal with the gradient of the Gaussian operator, $g(x; \sigma)$. The set containing multiscale edges, $E=\{e_1, e_2, \ldots, e_n\}$, can be obtained by registering the maxima in w_i, since a high gradient value indicates a sharp change at that point. Alternatively, the sets V and W can be constructed using regularization. In this case, given a set of regularization parameters, $L = \{\lambda_1, \lambda_2, \ldots, \lambda_n\}$, with $\lambda_1<\lambda_2<\ldots<\lambda_n$, the set V is constructed by $V = \{v_{\lambda_1}, v_{\lambda_2}, \ldots, v_{\lambda_n}\}$, where

$$v_{\lambda_i} = v(x; \lambda_i) = \{v(x) : E(v) = \inf_{f \in V} \int_{\mathbb{R}} [(f - d)^2 + \lambda_i^2 (\frac{\partial f}{\partial x})^2] dx\}.$$

which is the function that minimizes the string functional with the regularization parameter λ_1^2. The set W is constructed from the gradient of the function v_{λ_i}. The Euler-Lagrange equation associated with the string functional is

$$f - d - \lambda \frac{\partial^2 f}{\partial x^2} = 0$$

with the boundary conditions

$$\frac{\partial f}{\partial x}\Big|_{-a,b} = 0 .$$

The solution satisfying the boundary conditions is given by [BLAK 87]

$$f(x) = \int_{-a}^{b} G(x, x')\, d(x')\, dx'$$

where G(x,x') is the Green's function. For a bi-infinite domain ($a, b \to \infty$),

$$G(x, x') = \frac{1}{2\lambda} e^{-|x-x'|/\lambda}.$$

and thus the solution can be written as

$$f(x) = \int_{-\infty}^{\infty} \frac{1}{2\lambda} e^{-|x-x'|/\lambda}\, d(x')\, dx' ,$$

which is the convolution of the data d with a filter whose impulse response is

$$h_r(x; \lambda) = \frac{1}{2\lambda} e^{-|x|/\lambda}$$

where λ controls the effective size of the filter so that a small λ causes a

small degree of smoothing. Thus a multiscale representation $V=\{v_{\lambda_1}, v_{\lambda_2}, \ldots, v_{\lambda_n}\}$ can be constructed by computing v_{λ_i} as

$$v_{\lambda_i} = d * h_r(x; \lambda_i)$$

where $h_r(x; \lambda_i)$ is the first order regularization filter. The set W can be constructed by convolving the signal with the derivative of $h_r(x; \lambda_i)$;

$$w_i = \frac{d}{dx} (d * h_r(x, \lambda_i)) = d * g_r(x, \lambda_i) .$$

where

$$g_r(x; \lambda) = \frac{d}{dx} h_r(x, \lambda) = \frac{-1}{2\lambda^2} \frac{x}{|x|} e^{-|x|/\lambda} \qquad x \neq 0$$

which has a discontinuity at x=0.

It was shown that derivative of Gaussian is an optimal linear edge operator in terms of maximizing both good detection and good localization performance. This filter is localized both in spatial and frequency domains so that the ringing artifacts due to Gibbs phenemena are also minimized. Furthermore, Torre and Poggio [TORR 86] showed that minimizing the energy functional associated with a rod,

$$E_p(f, \lambda) = \int_\Omega (f - d)^2 \, dx + \lambda \int_\Omega f_{xx}^2 \, dx ,$$

is equivalent to convolving the data d with the cubic spline convolution filter named the second order R-filter which is very similar to Gaussian. Thus the filter h_r associated with minimizing the first derivative in $E_m(x,\lambda)$ rather than the second derivative in $E_p(x,\lambda)$ imposes a lower degree of smoothness as compared to the Gaussian. Indeed this filter favors the localization performance at the expense of degrading detection performance. In our study, the good localization performance of this filter is combined with the good detection performance attainable through utilizing the multiscale behavior of edges in multiscale representation.

Properties of the R-Filter and Its Relation with Other Edge Operators

A common approach in designing edge operators is to mathematically formulate the three edge detection criteria: good detection, good localization, and only one response to a single edge, and then to find a filter response which maximize them. Canny [CANN 86] formulated these three criteria as the signal-to-noise (SNR) ratio at the filter's output, the reciprocal of the root-mean squared distance of the marked edge from the

center of the true edge and the distance between adjacent maxima in the noise response of g respectively. These criteria are combined by maximizing the product of the first two criteria under the constraint of the third criterion. Canny approximated the solution of this constrained optimization problem by the first derivative of a Gaussian,

$$g(x) = - k \times e^{-x^2/2\sigma^2} .$$

As mentioned before, Torre and Poggio [TORR 86] followed a simple way, through minimization of the energy functional of a rod, to justify the use of the Gaussian-like operator as a smoothing operator prior to the differentiation. A similar filter was derived by Deriche [DERI 87][DERI 90] by extending the Canny's filter to the range $[-\infty, \infty]$. This modification leads to an approximate solution

$$g(x) = k \times e^{-\alpha|x|},$$

which can be recursively implemented and performs better than Canny's operator. Shen and Casten [SHEN 86] deduced a smoothing operator prior to differentiation by minimizing a combined criterion,

$$C = \sqrt{E_N E_{N_x} / E_S}$$

where E_N is the noise energy at the output of smoothing filter, E_{N_x} is the noise energy of the first derivative of the filter output and E_S is the first derivative of the response to the step edge. The filter response which maximizes this combined criterion is given as

$$h(x) = k \, e^{-p|x|} \qquad \text{with } p>0.$$

This is the same as the regularization filter $h_r(x; \lambda)$ obtained from minimizing the string functional. This similarity can be justified because the criterion C imposes a high SNR for the first derivative of the filter's output, so does minimizing the string functional. Since the first derivative of this exponential filter is another exponential filter, it also satisfies the Canny's localization criterion. Shen and Casten used the zero crossing at the Laplacian of the image, which is approximated by taking difference between the input and output of this filter. Note that the third criterion for edge detection, one response to one edge, is not imposed in obtaining the Shen and Casten's filter or the first order R-filter. This results in a filter which is less regular as compared to Canny's and Deriche's optimal filters or the second order R-filter associated with a rod functional.

Gokmen [GOKM 90b] used another edge operator based on the R-filter $h_r(x;\lambda)$; this operator is based upon the zero crossing in the Difference of Regularized Solutions (DORS) obtained with two different regularization parameters λ_1 and λ_2. The DORS filter $DORS(x,\lambda_1,\lambda_2)$ is given by

$$DORS(x;\lambda_1,\lambda_2) = h_r(x;\lambda_1) - h_r(x;\lambda_2) .$$

In the Gaussian case, it is well known that the Laplacian of a Gaussian can be approximated by the difference of two Gaussians up to a constant. However, $DORS(x;\lambda,\lambda+\delta\lambda)$ is not the Laplacian of $h_r(x;\lambda)$; indeed,

$$\lim_{\delta\lambda\to 0} DORS(x;\lambda,\lambda+\delta\lambda) = \lim_{\delta\lambda\to 0} (h_r(x;\lambda) - h_r(x;\lambda+\delta\lambda))$$

$$\approx \delta\lambda \frac{\partial}{\partial\lambda} h_r(x;\lambda) \approx k_1\left(1 - \frac{|x|}{\lambda}\right) e^{-|x|/\lambda} .$$

Let a new filter $h(x;\lambda)$ be constructed,

$$h(x;\lambda) = k_2 \left(1 + \frac{|x|}{\lambda}\right) e^{-|x|/\lambda} ,$$

such that its gradient is

$$\frac{\partial}{\partial x} h(x;\lambda) = -\frac{k_2}{2\lambda} x\, e^{-|x|/\lambda}$$

and its Laplacian is the limit of $DORS(x;\lambda,\lambda+\delta\lambda)$. The gradient of the filter $h(x;\lambda)$ is the same as the Deriche's optimal filter up to a constant. As indicated before, Deriche's filter is similar to the first derivative of a Gaussian and the R-filter obtained by minimizing a rod functional. This implies that even though the R-filter $h_r(x;\lambda)$ has low regularity, a higher degree of regularity can be achieved by using the difference of two such filters with different scale parameters as utilized in reference [GOKM 90b]. Because of this important property, one can efficiently achieve a higher degree of regularity from less regular but computationally more efficient solutions.

Experimental Results

When an image is scanned line by line, its 1-D profiles can be decomposed into different frequency channels using the R-filter $h_r(x;\lambda)$. In our experiments, four dyadic scale parameter values were used, $\lambda_i = 2^{i-1}$, $(i=1,2,3,4)$. The linear size of the filter was chosen as 8λ which possesses 98.2% of the entire area under the function $h_r(x,\lambda)$. Fig. 2.1(a) shows a noisy profile extracted from an image with SNR=7 db. The lower four signals show the multiscale representation v_1, v_2, v_3 and v_4. A coarser description

is obtained as the value of the scale parameter increases. Fig. 2.1(b) shows the noisy data at top followed by gradient signals at different scales constructing the set W; w_1, w_2, w_3 and w_4. The edge signals at different scales, called the E set, are obtained by keeping only the maxima in the W set, and they are shown in Fig. 2.1(c). As expected, noisy edges gradually disappear at coarse scales while the locations of the remaining edges are as accurate as those in the fine scales. Because of this spatial coincidence of edges at different scales, these multiscale edges can be combined by a simple integration scheme. To explore the localization and detection performances, the one dimensional filter $g_r(x; \lambda_1)$ was applied to rows and columns of an image. The result showed that this edge operator can extract the accurate edge locations even if the nearby edges may interact and can also extract sharp corners without smoothing them.

The edges obtained in different scales can be integrated by using the following scheme. From the edges detected at all scales, the following edge pixels are to be erased: those isolated in all scales, those isolated in coarse scales but disappeared in a fine scale, and those presented only in a single scale and isolated. This rule allows us to partially eliminate those isolated edges which are not connected to any other edge point but appear only in the fine scale. The experimental result on applying this algorithm to a girl's image (Lenna image) is shown in Fig. 2.2. The edges detected at different scales are shown in Fig. 2.2(a) and the combined edges as well as original image are shown in Fig. 2.2(b). Some of the details and textures disappearing in coarse scales were captured by the integration scheme.

The work planned for the second year is to explore the possible combination of the first and second order R-filters for accurate edge detection, and to study the relationship between regularization theory and wavelet theory. A wavelet representation of an image will be constructed using recursive H and G filters related to h_r and g_r (or h and g) used in this regularization based algorithm.

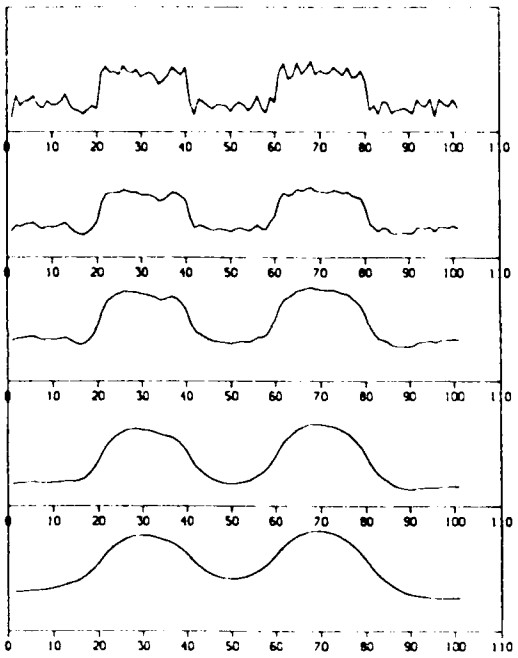

(a)

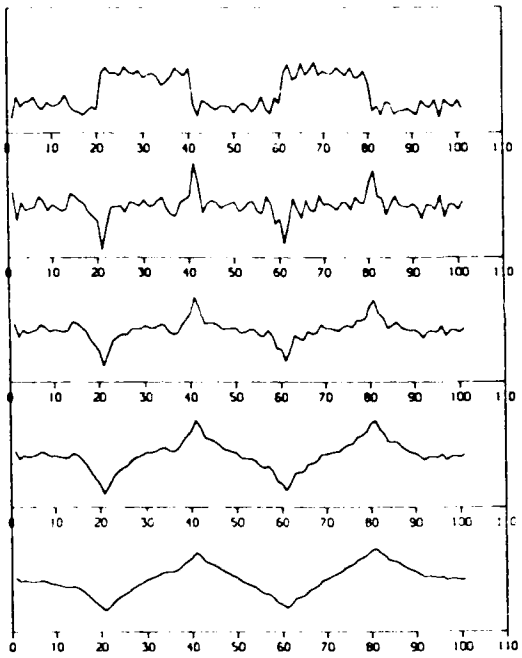

(b)

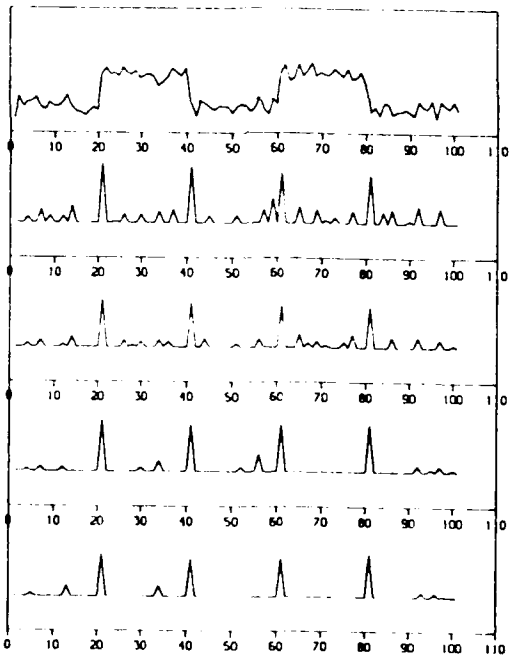

(c)

Figure 2.1 The profile from a checkerboard image with SNR=7dB: (a) The set V with, from top to bottom: original signal d, v_1, v_2, v_3 and v_4; (b) The set W with, from top to bottom: d, w_1, w_2, w_3 and w_4; (c) The set E with, from top to bottom: d, e_1, e_2, e_3 and e_4.

(a)

(b)

Figure 2.2 The multiscale edges from the Lenna image: (a) the images at different scales (b) the original image and the combined edges.

B.3. Parallel Image Processing

In the first year of the project a set of endeavors has been undertaken to develop a deeper appreciation of the application of parallel processing approaches to image processing. In particular the potential for wavelet transform applications has spurred interest in embedding of wavelet transformed images into 2-D mesh architectures and in the closely related problem of embedding pyramid architectures into meshes in order to efficiently perform multiresolution processing. Different embeddings of the wavelet transform coefficients into 2-D meshes have been considered and the time performances of these embeddings have been evaluated for typical algorithms central to wavelet transform applications. The application of reconfigurable meshes for pyramid emulation has been considered and a range of potential computational models has been identified. In order to fully utilize the potential of these various mesh computing models image processing algorithms is under study to enable their fully parallel application in the given target architecture and where possible to identify fundamental limits of parallel algorithms, e.g. required support size or communication demands. The identification of fully (or near fully) parallel multiresolution approaches has been identified as a key goal for the second year of the project. Finally, several novel graph compounds have been studied which can be utilized to enhance communication bandwidth in mesh architectures and may offer some promise in image processing. In the following some further detail is given regarding these endeavors and their rationale.

B.3.a. Parallel Computations for Wavelet Transforms

Multiresolution image processing is typically a natural fit to pyramid computing architectures. [AHUJ 84], [BURT 83], [TANI 83] Wavelet forms of image representation for n by n images can place a multiresolution representation into an n by n mesh architecture with one coefficient per processing element (PE) [MALL 89a]. Examples of such mesh architectures are available [DUFF 86], [KITT 85], [FOUN 90] and are likely to be more readily available than pyramid architectures in the future. Thus, n by n mesh architectures might be desirable targets for wavelet based algorithm development. A key issue in utilizing such mesh architectures is the determination of where in the mesh the wavelet transform coefficients are stored. Different "embeddings" of the wavelet transform coefficients in the mesh have been considered and their performances on basic transform

algorithms have been evalutated. Some typical results are illustrated below.

In this presentation 2 embeddings are considered as illustrated in Figure 3.1. In the following the original image is thought of as level 0 and successive levels, i = 1, 2, ..., refer to the successively lower resolution image representations characteristic of the wavelet transform. In the embedding illustrated in Figure 3.1(a) (following [MALL 89a]) the detail images D_i^1, D_i^2 and D_i^3 at level i of the multiscale transform and the lower resolution version of the image, A, are concentrated into subblocks within the mesh. This embedding is denoted Block-Concentrated (**BC**). A second embedding has been developed, denoted Distributed (**Dist**), and is illustrated in Figure 3.1(b) where the individual components of A, a, and the individual components of the detail images at level i, d_i^1, d_i^2 and d_i^3, are distributed over the mesh. Specific detail image components at level i (i>0) corresponding to the same base image location are mapped to PE's in the mesh which are 2^i distance apart for the **Dist** case and 2^{n-i+1} distance apart for the **BC** case. Thus, **BC** has higher communication cost at lower levels and lower communication cost at higher levels while the opposite holds for **Dist**.

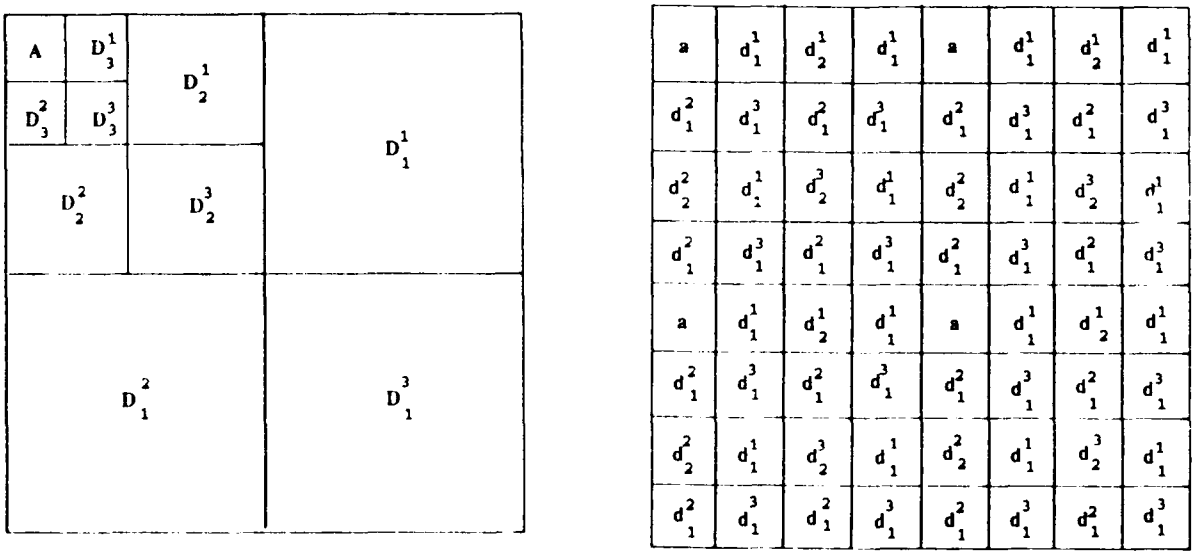

(a) (b)

Figure 3.1 Wavelet transform embeddings in a 2-D mesh architecture: (a) Block-Concentrated embedding (**BC**); (b) Distributed (**Dist**) embedding.

Time performance results are reported here for algorithms which decompose a given image into its wavelet transform and reconstruct the original image from its wavelet transform. The decomposition process requires a set of linear convolutions along rows and columns of the mesh with special data movements to place the results in the desired locations. The reconstruction process requires the insertion of rows and columns of zeros in the mesh, row and column linear convolutions, and data movements to restore image components to their original locations. The mesh model used in this analysis includes 4-neighbors connections and "wrap-around" connections for rows and columns. (This form of 2-D mesh interconnection is sometimes referred to as a torus) The convolution algorithm used in this analysis follows [RANK 90]. Only the communication steps (e.g. movements of data from PE to neighboring PE) are evaluated in this analysis since both embeddings require the same number of computation steps. (e.g. adds and multiplies within a given PE) The number of communication steps required for each algorithm over each embedding have been evalutated in closed form. Some typical results are illustrated in Tables 3.1 and 3.2 for a filter size of 8. In each table the results are normalized by expressing number of communication steps as a multiple of the linear dimension of the image, n. In Table 3.1 the wavelet transforms are computed to a level where the lowest resolution image is the size of the filter, i.e. 8 for these results. In Table 3.2 the transforms are performed only to 3 levels of resolution for each image space size. In the former case more processing at higher levels of the multiresolution structure is required than in the latter case. In multiresolution processing where lower numbers of levels of resolution are used the Table 3.2 data is more representative and where larger numbers of levels of resolution are required the Table 3.1 data is more representative.

Table 3.1 Communication Steps Required by Wavelet Decomposition/ Reconstruction Algorithms Taken to/on 8x8 Lowest Resolution Images (Filter size is 8)

Image Size n x n	Decomposition		Reconstruction	
	BC	**Dist**	**BC**	**Dist**
1024 x 1024	8.4 n	9.2 n	4.4 n	14.1 n
512 x 512	8.7 n	9.3 n	4.7 n	14.3 n
256 x 256	9.2 n	9.6 n	5.2 n	14.5 n
128 x 128	9.9 n	9.9 n	6.0 n	14.8 n
64 x 64	11.0 n	10.4 n	7.2 n	15.1 n

Table 3.2 Communication Steps Required by Wavelet Decomposition and Reconstruction Algorithms Working on Images of only 3 Levels of Resolution (Filter size is 8)

Image Size n x n	Decomposition		Reconstruction	
	BC	**Dist**	**BC**	**Dist**
1024 x 1024	6.1 n	.34 n	3.6 n	.47 n
512 x 512	7.3 n	.67 n	3.8 n	.95 n
256 x 256	7.6 n	1.36 n	4.1 n	1.9 n
128 x 128	8.3 n	2.70 n	4.8 n	3.8 n
64 x 64	9.6 n	5.40 n	6.1 n	7.6 n

In Table 3.1 data, where higher level processing is required, **Dist** typically requires greater communication overhead than **BC**. These observations are largely reversed for the Table 3.2 data where the processing is restricted to a fixed number of levels. Thus, where one can avoid building a multiresolution representation with a large number of levels the **Dist** embedding appears to offer some promise as a time efficient wavelet embedding for mesh architectures. This investigation is on-going with the consideration of other embeddings, e.g. [STOU 88], and a greater variety of parallel vision algorithms. This work contributes to research objective A.2.b.

B.3.b. **Reconfigurable Mesh Architectures for Multiresolution Processing**

Although the embedding of a problem in the mesh can be fine-tuned to enhance performance, multiresolution processing presents fundamental tradeoffs in the mesh: In **BC** type embeddings good time performance **within** levels tends to produce poor time performance **across** levels or for distributed type embeddings one cannot get both good performance in the base and at high levels. Of course, a fully realized pyramid architecture can eliminate this problem, but the mesh has a more desirable VLSI layout. Reconfigurable mesh architectures [LIST 91] suitable for use in image processing are currently in development and offer very desirable characteristics for multiresolution processing. The PAPIA2 architecture [CANT 88], [ALBA 91] is essentially an 8-connected mesh with the capability of bypassing PE's in the mesh to enable direct connections with distant PE's. Figure 3.2 illustrates an embedding of a 6 level pyramid in a PAPIA2 style mesh of size 32x32. Each mesh PE emulates 1 pyramid base PE and at most 1 pyramid PE above the base. PE's labeled + emulate only the base whereas PE's labeled i emulate a pyramid PE in level i. PAPIA2 reconfigurability allows PE's emulating each level above the base to communicate directly with their 4-neighbors without contention. Thus, it is theoretically possible to have levels above the base operating in parallel. Through such reconfigurations the fundamental tradeoffs in pyramid embedding in the mesh, mentioned in the previous section, are alleviated as all neighbors in a pyramid can be configured to be neighbors in this mesh, albiet not simultaneously.

The polymorphic torus, developed at IBM, [MARE 91] is a somewhat more powerful reconfigurable mesh and motivates the following model for the primary mesh architecture to be utilized in algorithm development in the second year of the project. Figure 3.3 illustrates a 4x4 piece of this model where each position of the mesh is occupied by a PE and a Switch. Each PE is 4-connected to other PE's with a traditional mesh interconnection and its associated switch handles interaction with separate row and column busses. Figure 3.4 illustrates some of the possible configurations of the switches. By allowing for up to 4 independent connections between PE's and associated switches, the PE's can utilize the row and column busses to form 4 direct connections with PE's along the same row and column. Using the same embedding of the pyramid into the mesh as illustrated in Figure 3.2,

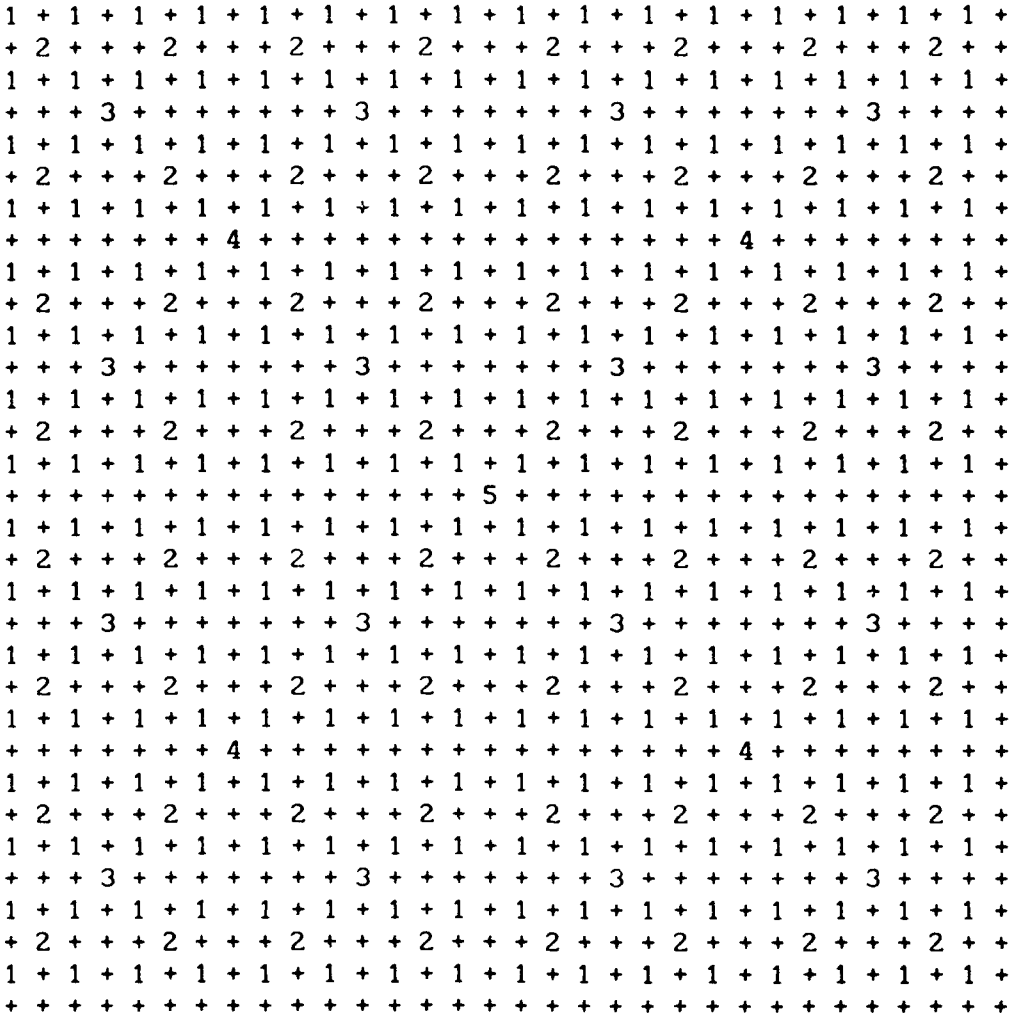

Figure 3.2 Embedding of a 6-level pyramid in a 32x32 mesh. Symbols + represent mesh PE's realizing only a pyramid base PE and integers i represent PE's realizing a base PE and level i PE in the pyramid.

each pyramid level above the base is able to function independently with direct connections to 4-neighbors within each pyramid level provided by segments of the row and column busses. Furthermore, by emulating 2 image pixels within every other "+" PE and by providing bypass capability, within PE's, of the PE mesh connections, the base of the pyramid can be emulated in parallel with all levels above. In this model a certain degree of PE autonomy [FOUN 90] will be assumed whereby PE's in different levels can perform different instructions in parallel. Also, a global "wired or" bus is assumed to be available. Variations on this model for a reconfigurable mesh will be used in studies of parallel algorithm development in the second year of the project. The potential of 3-D meshes, with and without

reconfigurability, will also be investigated. This work contributes to research objective A.2.a.

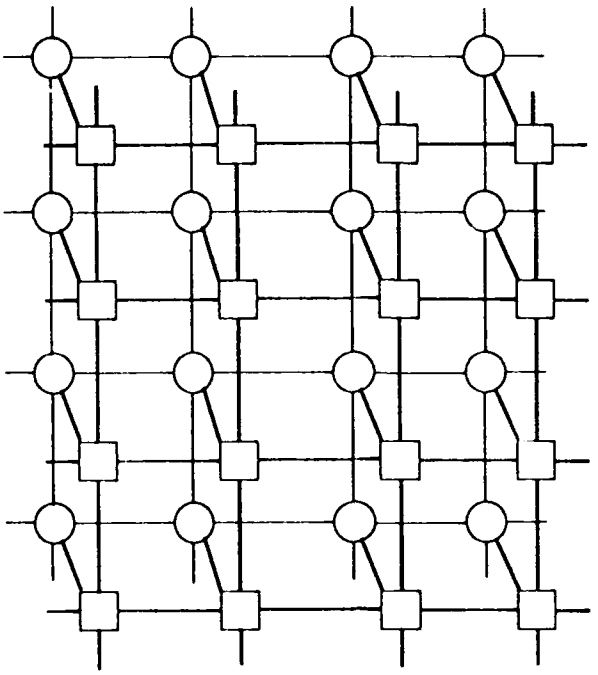

Figure 3.3 A 4x4 piece of a reconfigurable mesh model. Circles represent PE's and squares represent switches.

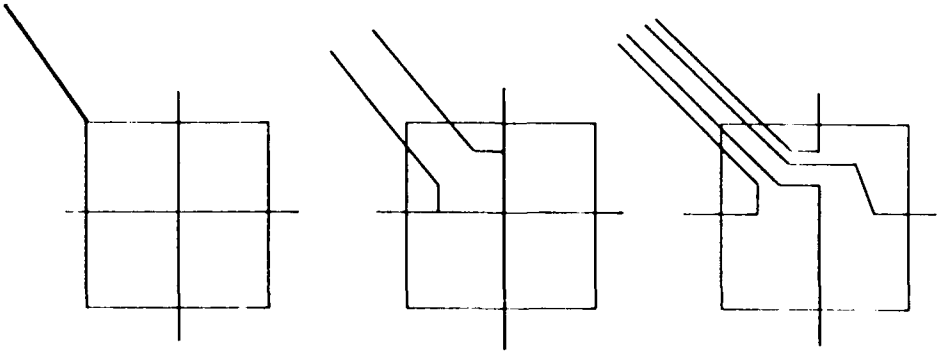

Figure 3.4 Typical switch settings for the reconfigurable mesh model. In (a) the PE is disconnected from row and column busses; in (b) the PE is able to communicate on row and column busses independently; and in (c) the row and column busses are opened and the PE communicates along each bus segment independently.

B.3.c. **Fully Parallel Algorithms**

It is a fundamental goal in the application of parallel computing to make algorithms as fully parallel as possible in order to utilize the potential of a large number of processors. To achieve this one must develop a deep understanding of the communication demands and fundamental nature (e.g. required support sizes, potential for fully parallel operation with limited supports, etc.) of the particular algorithms under study. In typical applications of pyramid or multiresolution algorithms serial application of processing within individual levels is used with results from one level used to affect processing in succeeding levels. Thus, many processors in the pyramid are idle at any one time. Given the kind of pyramid emulation model envisioned in the previous section it is desirable to develop pyramid algorithms which can operate fully in parallel making simultaneous use of all or a large number of levels. Multiresolution approaches will be considered for a variety of problems including wavelet-based boundary identification, skeletonization in binary and gray level images, connected component labeling for binary images and graphs, matrix multiplication, template matching, Generalized Hough approaches for object recognition, etc. This investigation will be a main theme of the project in the second year and will contribute to research objectives A.2.c, A.2.d, and A.3.

Fundamental limitations on fully parallel applications of certain connectivity preserving "reduction-only" operators, with applications in 2-D thinning, have been studied in the past year. [Hall 91] (See [GOKM 90a] and PRES 84] for definitions and examples of reduction and augmentation operators) The size and strict limitations on the locations of optimally small supports for 2-D thinning operators have been identified which allows the algorithm designer to focus on a relatively small set of possible optimally small support "shapes". Similar investigations are on-going in studies of reduction-only parallel processes in 3-D image spaces and in reduction/augmentation processes in 2-D and 3-D spaces. The design of multiresolution transformations which preserve all or part of the connectivity properties of the original image are currently under investigation with the hope of developing fully parallel multiresolution connectivity preserving reduction and/or reduction/augmentation operators. Such operators will help to form fundamental building blocks in fully parallel multiresolution processing. This work should also produce results

or tests useful for verifying connectivity preservation for multiresolution algorithms. This work contributes to research objective A.2.d.

B.3.d. **Compound Graph Networks for Enhancing Mesh Communication**

Although the pyramid emulations discussed earlier are a very promising cost-effective approach, pyramids have fundamental limitations when processing demands are strongly global [Stou 86] as for sorting or many Hough transform applications. In these cases the pyramid connectivity (and that for the associated reconfigurable meshes emulating the pyramid) is inadequate slowing performance to that comparable to a mesh alone. Thus, in applications where better time performance is needed on strongly global tasks, networks with higher connectivity are desirable. The well-known binary hypercube is a powerful highly connected network useful for stongly global computations, but is relatively expensive to build in large instances. Certain forms of graph compounds have been identified which can produce performance approaching the hypercube but with substantially reduced hardware cost. (or network degree) [HAMD 90], [HAMD 91a], [HAMD 91b] These graph compounds can be used to augment communication capability in a mesh to help achieve higher performance.

The RGC network proposed in [HAMD 91b] is a constant degree network which is envisioned as an augmentation of a traditional 2-D mesh architecture. The RGC is formed by compounding a given number of atom graphs with a complete interconnection and this compounding is done for any desired number of levels. An example is illustrated in Figure 3.5 where the atom graph is a binary hypercube. (referred to as an RGC-CUBE) Table 3.3 illustrates the comparative asymptotic performance on various basic image processing algorithms (operating on an nxn image of size $N=n^2$ pixels) for two instances of an RGC-CUBE as compared to the 2-D mesh, pyramid, Mesh of Trees (MOT) [NATH 83] and Mesh with global mesh (MGM) [CARL 88], [PRAS 89]. These results are not bad and RGC-CUBE appears to offer some potential in image processing, but most of the algorithms studied do not fully utilize the full interconnection capability of the RGC-CUBE. Research is on-going to more fully exploit this useful network and particular emphasis is being given to the RGC-TREE instance where the atom graph is a binary tree. In this instance the RGC-TREE appears to be somewhat more powerful than MOT but with substantially fewer PE's. This RGC instance appears to offer particularly good potential for multiresolution processing. This work contributes to research objectives A.2.a. and A.2.d.

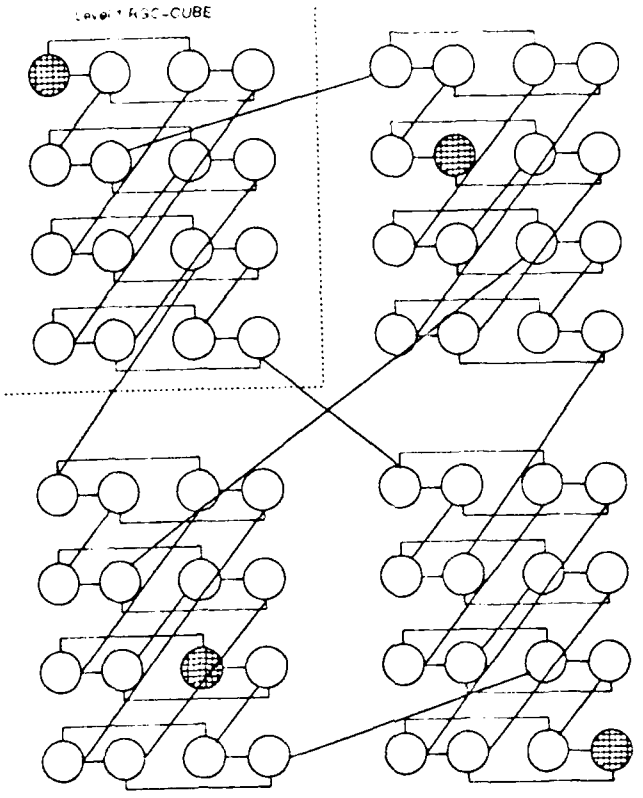

Figure 3.5 A 64-node example of a 2-RGC-CUBE. Shaded nodes (PE's) are available for expansion to higher level netwo[illegible].

Table 3.3 Asymptotic Time Complexities for Several Architectures for a Variety of Fundamental Image Processing Algorithms

Network	Mesh	Pyramid	MOT	MGM	2-RGC-CUBE	3-RGC-CUBE
Global Maxima	$O(N^{1/2})$	$O(\log(N))$	$O(\log(N))$	$O(N^{1/4})$	$O(\log(N))$	$O(\log(N))$
Connected Component Labeling	$O(N^{1/2})$	$O(N^{1/4})$	$O(\log^3(N))$	$O(N^{1/4}\log^2(N))$	$O(N^{1/6}\log(N))$	$O(N^{1/4}\log(N))$
Convex Hull	$O(N^{1/2})$	$O(\log^2(N))$	$O(\log(N))$	$O(N^{1/4})$	$O(N^{1/6}\log(N))$	$O(N^{1/4}\log(N))$
Diameter	$O(N^{1/2})$	$O(N^{1/4}\log(N))$	$O(\log(N))$	$O(N^{1/4})$	$O(N^{1/6}\log(N))$	$O(N^{1/4}\log(N))$
Smallest Enclosing Rectangle	$O(N^{1/2})$	$O(N^{1/4}\log(N))$	$O(\log(N))$	$O(N^{1/4})$	$O(N^{1/6}\log(N))$	$O(N^{1/4}\log(N))$
Smallest Enclosing Circle	$O(N^{1/2})$	$O(N^{1/4}\log(N))$	$O(\log(N))$	$O(N^{1/4})$	$O(N^{1/6}\log(N))$	$O(N^{1/4}\log(N))$

The RCC class of interconnection networks is another form of complete graph compound, but with substantially greater bandwidth and node degree which grows with network size. [HAMD 90] The RCC-CUBE instance in this class is able to efficiently emulate binary hypercube and achieves time performance very close to hypercube on a variety of strongly global algorithms, i.e. sorting and PRAM emulation, while maintaining a substantially lower degree and hardware cost. The RCC-FULL instance [HAMD 91b] is able to outperform binary hypercube by performing sorting and PRAM emulation in O(logN) time while still maintaining a reduced node degree as compared to hypercube. These high connectivity networks appear to be promising cost-effective alternatives to binary hypercube when strongly global problems must be solved. The application of these networks for supporting a variety of Generalized Hough transform approaches is currently under study. This work contributes to research objectives A.2.a. and A.2.d.

C. RESEARCH ARTICLES

[1] "Edge Detection Using Refined Regularization," M. Gokmen and C.C. Li, Proceedings of the IEEE Computer Society Conference on Computer Vision and Pattern Recognition, 1991, pp. 215 221; a revised version will be submitted to IEEE Trans. on Pattern Analysis and Machine Intelligence. (Our Electrical Engineering Department, Technical Report, TR-SP-91-02, April 1991).

[2] "The Split Dyadic Wavelet Transform for Signal Analysis," M. Sun, C.C. Li and R.J. Scalabassi, submitted to IEEE Trans. on Signal Processing. (Our Electrical Engineering Department, Technical Report, TR-SP-91-03, May 1991).

[3] "Multiscale Edge Detection Using First Order R-Filter," M. Gokmen and C.C. Li, will be submitted to IEEE Trans. on Pattern Analysis and Machine Intelligence. (Our Electrical Engineering Department, Technical Report, TR-SP-91-04).

[4] "Optimally Small Operator Supports for Fully Parallel Thinning Algorithms," R.W. Hall, submitted to IEEE Trans. PAMI, 1991. Also available as technical report TR-SP-91-01, Department of Electrical Engineering, University of Pittsburgh.

[5] "Recursively Generated Complete Graph Compounds: Efficient Networks for Parallel Computations," M. Hamdi and R.W. Hall, submitted to IEEE Trans. Computers, 1990 (revised May 1991). Also available as technical report TR-CE-90-02, Department of Electrical Engineering, University of Pittsburgh.

[6] "RCC-FULL: An Effective Network for Parallel Computations," M. Hamdi and R.W. Hall, submitted to J. of Parallel and Distributed Computing, 1991. Also available as technical report TR-CE-91-03, Department of Electrical Engineering, University of Pittsburgh.

[7] "Parallel Image Computations on Meshes Augmented with Compound Graphs," M. Hamdi and R.W. Hall, in preparation.

[8] "Embedding Wavelet Transforms in Parallel Architectures," M. Hamdi and R.W. Hall, in preparation.

D. PARTICIPATING PROFESSIONAL PERSONNEL

Professor Ching-Chung Li, Co-Principal Investigator
Professor Richard W. Hall, Co-Principal Investigator
Dr. M. Gokmen, Post-doctoral Research Fellow
H.J. Kim, Graduate Research Assistant
M. Hamdi, Graduate Research Assistant
W.K. Kim, Teaching Fellow

E. INTERACTIONS

Professor Li attended the NSF/CBMS Conference on Wavelets held at University of Lowell, Lowell, MA, June 11-15, 1990, and also the AFIT/AFOSR Symposium on Applications of Wavelets to Signal Processing, held at AFIT, Wright-Patterson Air Force Base, OH, March 20-22, 1991. Both Professor Li and Professor Hall attended the DARPA Image Understanding Workshop, Pittsburgh, PA, September 11-13, 1990.

Professor Li, Professor Hall and Dr. Gokmen attended the IEEE Computer Society Conference on Computer Vision and Pattern Recognition, Maui, HI, June 4-6, 1991. A paper entitled "Edge Detection Using Refined Regularization" was presented at the conference.

Our research group has been in interaction with Professors K.S. Lau, C.J. Lennard and J.J. Manfredi of our Mathematics Department. They conducted a series of seminars on wavelet theory during the Fall and Spring Terms, 1990-91.

F. REFERENCES

[AHUJ 84] N. Ahuja and S. Swamy, Multiprocessor pyramid architectures for bottom-up image analysis, IEEE Trans. Pattern Anal. and Mach. Intell., PAMI-6, 1984, 463-475.

[ALBA 91] M.G. Albanesi, V. Cantoni, U. Cei, M. Ferretti and M. Mosconi, Embedding pyramids into mesh arrays, in [LIST 91].

[BARL 91] M. Barlaud, T. Gaidon, P. Mathieu and J.C. Feauveau, Edge Detection Using Recursive Biorthogonal Wavelet Transform, Proc. IEEE International Conference on Acoustics, Speech, and Signal Processing, May 1991, 2553-2556.

[BLAK 87] A. Blake and A. Zisserman, Visual Reconstruction, MIT Press, 1987.

[BURT 83] P.J. Burt, The pyramid as a structure for efficient computation, in A. Rosenfeld, ed., Multi-Resolution Systems for Image Processing, 1983.

[CANN 86] J.F. Canny, A Computational Approach to Edge Detection, IEEE Trans. Pattern Anal. Mach. Intell., Vol. PAMI-8, 1986, 679-698.

[CANT 88] V. Cantoni and S. Levialdi, Multiprocessor computing for images, Proc IEEE, 76, 1988, 959-969.

[CARL 88] D.A. Carlson, Modified mesh-connected parallel computers, IEEE Trans. Computers, C-37, 1988, 1315-1321.

[CHAN 90] A.K. Chan and C.K. Chui, Real-Time Signal Analysis with Quasi-interpolatory Splines and Wavelets, CAT report 221, Center for Approximation Theory, Department of Mathematics, Texas A&M University, July 1990.

[DERI 87] R. Deriche, Optimal Edge Detection using Recursive Filtering, Proc. First Int. Conf. Computer Vision, 1987, 501-505.

[DERI 90] R. Deriche, "Fast Algorithms for Low-Level Vision, IEEE Trans. Pattern Anal. Mach. Intell., Vol. 12, 1990, 78-87.

[DAUB 88] I. Daubechies, Orthonormal Bases of Compactly Supported Wavelets, Comm. on Pure and Applied Math., Vol. 91, 1988, 906-996.

[DUFF 86] M.J. B. Duff and T.J. Fountain, Eds., Cellular Logic Image Processing, New York: Academic Press, 1986.

[FOUN 90] T.J. Fountain, The CLIP7 Programme, in Multiprocessor Computer Architectures, T.J. Fountain and M.J. Shute, eds., North-Holland, Amsterdam, 1990.

[GOKM 90a] M. Gökmen and R. W. Hall, Parallel shrinking algorithms using 2-subfields approaches, Computer Vision Graphics Image Process., 52, 1990, 191-209.

[GOKM 90b] M. Gokmen, Edge Detection Using Regularization Theory, PhD dissertation, University of Pittsburgh, 1990.

[GOKM 91] M. Gokmen and C. C. Li, Multiscale Edge Detection Using First Order R-filter, Tech. report, University of Pittsburgh, TR-SP-91-04, June, 1991.

[HALL 91] R.W. Hall, Optimally small operator supports for fully parallel thinning algorithms, submitted for publication, 1991. Also available as technical report TR-SP-91-01, Department of Electrical Engineering, University of Pittsburgh.

[HAMD 90] M. Hamdi and R.W. Hall, Recursively generated complete graph compounds: Efficient networks for parallel computations, submitted for publication, 1990. Also available as technical report TR-CE-90-02, Department of Electrical Engineering, University of Pittsburgh.

[HAMD 91a] M. Hamdi and R.W. Hall, RCC-FULL: An effective network for

parallel computations, submitted for publication, 1991. Also available as technical report TR-CE-91-03, Department of Electrical Engineering, University of Pittsburgh.

[HAMD 91b] M. Hamdi, Communication-Efficient Interconnection Networks for Parallel Computations, PH.D. Dissertation, University of Pittsburgh, Department of Electrical Engineering, 1991.

[KITT 85] J. Kittler and M.J.B. Duff, Image Processing System Architectures, John Wiley, New York, 1985.

[LIST 91] H. Li and Q.F. Stout, eds. Reconfigurable Massively Parallel Computers, Prentice Hall, Englewood Cliffs, New Jersey, 1991.

[LUJA 89] Y. Lu and R.C. Jain, Behavior of Edges in Scale Space, IEEE Trans. Pattern Anal. Mach. Intell., Vol. 11, 1989, 337-356.

[MALL 89a] S.G. Mallat, A theory for multiresolution signal decomposition: the wavelet representation, IEEE Trans. Patt. Anal. Mach. Intell., 11, 1989, 674-693.

[MALL 89b] S.G. Mallat and S. Zhong, Complete Signal Representation with Multiscale Edges, TR No. 483, Department of Computer Science, Courant Institute of Mathematical Sciences, New York University, December 1989.

[MALL 91] S.G. Mallat and S. Zhong, Wavelet Transform Maxima and Multiscale Edges, in Wavelets and Applications, Eds., R. Coifman, et al., Jones and Bartlett, 1991.

[MARE 91] M. Maresca and H. Li, Polymorphic VLSI arrays with distributed control, in [LIST 91].

[NATH 83] D. Nath, S.N. Maheshwari and P.C.P. Bhatt, Efficient VLSI networks for parallel processing on orthogonal trees, IEEE Trans. Computers, C-32, 1983, 569-581.

[PENT 90] A. Pentland, Finite Element and Regularization Solutions Using Wavelet Bases, Tech. Report No. 143, Media Lab. Vision and Modeling Group, MIT, June 1990.

[PRAS 89] V.K. Prasanna-Kumar and D. Reisis, Image computations on meshes with multiple broadcast, IEEE Trans. Pattern Anal and Mach. Intell., PAMI-11, 1989, 1194-1202.

[PRES 84] K. Preston and M.J.B. Duff, Modern Cellular Automata, Plenum, New York, 1984.

[RANK 90] S. Ranka and S. Sahni, Convolution on mesh connected multicomputers, IEEE Trans. Pattern Anal. and Mach. Intell., PAMI-12, 1990, 315-318.

[SHEN 86] J. Shen and S. Casten, An Optimal Linear Operator for Edge Detection, Proc. IEEE Conf. On Computer Vision and Pattern Recognition, 1986, 109-114.

[STOU 86] Q.F. Stout, Algorithms for meshes and pyramids, in Intermediate-Level Image Processing, M.J.B. Duff, ed., Academic Press, London, 1986.

[STOU 88] Q.F. Stout, Mapping vision algorithms to parallel architectures, Proc IEEE 76, 1988, 982-995.

[TAGA 90] H.D. Tajare and R.J.P. de Figueiredo, On the Localization Performance Measure and Optimal Edge Detection, IEEE Trans. Pattern Anal. Mach. Intell., 13, 1990, 1186-1190.

[TANI 83] S.L. Tanimoto, A pyramidal approach to parallel processing, Symp. Comp. Arch., ACM, 1983, 372-378.

[TORR 86] V. Torre and T. Poggio, On Edge Detection, IEEE Trans. Pattern Anal. Mach. Intell., Vol. PAMI-8, 1986, 147-163.

[ZETT 90] W. Zettler, J. Huffman and D.C.P. Linden, Application of Compactly Supported Wavelets to Image Processing, Tech. Report A-D 900119, AWARE, Inc., 1990.